

B. Delmonte · J. R. Petit · K. K. Andersen
I. Basile-Doelsch · V. Maggi · V. Ya Lipenkov

Dust size evidence for opposite regional atmospheric circulation changes over east Antarctica during the last climatic transition

Received: 18 September 2003 / Accepted: 2 April 2004 / Published online: 5 August 2004
© Springer-Verlag 2004

Abstract Three east Antarctic ice cores (Dome B, EPICA-Dome C and Komsomolskaia) give evidence for a uniform dust input to the polar plateau during the last glacial maximum (LGM)/Holocene transition (20 to 10 kyr BP) and the $^{87}\text{Sr}/^{86}\text{Sr}$ versus $^{143}\text{Nd}/^{144}\text{Nd}$ isotopic signature of the mineral particles highlights a common provenance from southern South America at that time. However, the size distribution of dust from the three ice cores highlights important differences within the east Antarctic during the LGM and shows clearly opposite regional trends during the climatic transition. Between Dome B and Dome C the timing of these changes is also different. A geographical diversity also arises from the different phasing of the short-term (multi-secular scale) dust size oscillations that are superposed at all sites on the main trends of glacial to interglacial changes. We hypothesize the dust grading is controlled by size fractionation in response to its atmospheric pathway, either in terms of horizontal trajectory or in altitude of transport. Such mechanism is supported also by the dust size changes observed during a volcanic event recorded in

Vostok ice. Ice core dust size data suggest preferential upper air subsidence over the EDC-KMS region and easier penetration of relatively lower air masses to the DB area during the LGM. At the end of the last glacial period and during the climatic transition the region of relatively higher subsidence progressively moved southward. The scenario proposed, supported also by the LGM/Holocene regional changes of snow accumulation, likely operates even at sub-millennial time scale.

1 Introduction

The Antarctic circumpolar vortex is one of the major components of the global atmospheric circulation; its variable strength, location and pattern result from the complex heat exchanges between the Antarctic ice cap, the sea ice and the circulation in the surrounding ocean (King and Turner 1997). The circum antarctic current, the deepwater formation in the Weddell Sea along with sea-ice formation are of primary importance and potentially imprint their own variability into the atmospheric circulation over the Antarctic and the circumantarctic (e.g. Van den Broeke 2000). The reconstruction of the past variability in the atmospheric transport of tracers such as aeolian dust of terrestrial origin is a first-order tool for documenting the atmospheric and climatic changes in the high latitudes of the Southern Hemisphere.

The paleo-dust cycle is documented today by many terrestrial, marine and polar proxies, especially for the Quaternary period (see Kohfeld et al. 2001, and references therein). Among the cold periods of the Pleistocene, the last glacial maximum (onwards LGM) has become a major focus for dust cycle modelling (Mahowald et al. 1999), largely because of the considerable amount of evidence documenting deposition rates and transport paths of windblown lithogenic material. Such estimates, moreover, are necessary for the evaluation of general circulations model (GCM) results.

B. Delmonte (✉)
Laboratoire de Glaciologie et de Géophysique de l'Environnement (LGGE-CNRS), BP96, 38402 Saint Martin d'Hères, France
E-mail: bdelmonte@nest.it

B. Delmonte · J. R. Petit · V. Maggi
University of Milano-Bicocca, Dipartimento Scienze Ambientali,
Piazza della Scienza 1, 20126 Milano, Italy

B. Delmonte
University of Siena, Department of Geological Science,
Via del Laterino 8, 53100 Siena, Italy

K. K. Andersen
Niels Bohr Institute for Astronomy, Physics and Geophysics,
University of Copenhagen, Denmark

I. Basile-Doelsch
IRD, BP 172, 97492 Sainte-Clotilde cedex, France

V. Ya Lipenkov
Arctic and Antarctic Research Institute,
38 Bering st, 199397 St Petersburg, Russia

The ca. 13 million km² wide Antarctic continent is still relatively poorly documented with respect to dust studies: the Byrd ice core (80°S, 120°W) provides the only west Antarctic dust record (Thompson and Mosley Thompson 1981), while for the east Antarctic dust concentration changes during the last climatic cycle are documented at low temporal resolution by the first Dome C ice core (*old* Dome C, 74°39'S, 124°10'E, Royer et al. 1983), the Vostok (78°28'S, 106°48'E) ice core (Petit et al. 1999), and the Dome B (77°05'S, 94°55'E) ice core (Jouzel et al. 1995). Recently, Delmonte et al. (2002a, b and in press) provided a new dust record for the last 220 kyr, which is particularly detailed for the last 27 kyr, from the EPICA-Dome C (EDC) ice core (75°06'S, 123°21'E), drilled within the framework of the European Project for Ice Coring in Antarctica.

The mineral dust archived in east Antarctic ice is exclusively aeolian and originates from the Southern Hemisphere continents (Basile et al. 1997). The short-term and long-term variations of its concentration and size distribution reflect several climatic and environmental factors such as soil surface properties at the source, meteorological conditions, the hydrological cycle and the removal processes occurring from the source to the sink, the atmospheric circulation and finally the snow accumulation at the deposition site.

Antarctic ice cores indicate that the atmospheric dust flux was higher by a factor ~10–30 during the last glacial with respect to the Holocene (Petit et al. 1981), probably in response to increased terrestrial aridity and more vigorous atmospheric circulation (Petit et al. 1999). A recent correlation between the Vostok and EDC dust concentration profiles over the last 220 kyr (Delmonte et al. in press) revealed that each ice core record is representative of the entire east Antarctic plateau in this respect.

Such a covariance between ice core dust records suggests a first-order uniformity in the dust input over east Antarctica and consequently in all parameters influencing dust flux (source strength, scavenging processes en route and transport conditions). Since these parameters are closely linked, some difficulties arise in isolating each of these processes. However, a parameter directly linked to the transport conditions and characteristics is the size distribution of microparticles (e.g. Ruth et al. 2003).

Dust size distribution changes provide therefore a powerful tool for the investigation and the assessment of the paleo-circulation dynamics. However, the reconstruction of atmospheric circulation variability is more complex for multiple sources located in different geographical regions. Therefore, the dust provenance has to be identified first; this is possible through the geochemical signature (⁸⁷Sr/⁸⁶Sr versus ¹⁴³Nd/¹⁴⁴Nd isotopes) of the mineral particles (Grousset et al. 1992; Basile et al. 1997).

The EDC dust size record for the last 27 kyr (Delmonte et al. 2002a, b) revealed some new aspects of the atmospheric circulation during the last climatic transi-

tion with respect to prior studies from other sites, showing finer dust particles during the LGM compared to the Holocene, while opposite results were obtained from the Vostok ice core (Briat et al. 1982). Moreover, the EDC dust size distribution record showed some short-term (millennial and secular scale) oscillations (Delmonte et al. 2002b) over the last 13 kyr, that were also found in a 7 kyr record from Vostok (Delmonte et al. submitted).

In this study we investigate the dust concentration and size distribution changes that occurred during the last climatic transition (from 10 to 20 kyr BP) over the 94°E–123°E sector of east Antarctica. Three ice cores have been studied (Fig. 1): Dome B (DB), Komsomolskaia (KMS) and EDC. Stable isotope analyses (Jouzel et al. 2001) indicate that the records encompass a major change in the Earth's climatic and environmental history: the last glacial period (or marine isotopic stage 2), the Last Glacial Maximum (LGM), the deglaciation (or termination 1), as well as the beginning of the Holocene. The pattern of the temperature changes deduced from stable isotopes for the last climatic transition, thoroughly documented for east Antarctica (see Jouzel et al. 2001), consists of a two-step process with two warming trends interrupted by the Antarctic cold reversal (ACR). Adopting the respective original chronologies for several ice cores in east Antarctica, Jouzel et al. (2001) found a considerable agreement among the records and a quasi-synchronicity of the changes.

In this work, beside the dust concentration and size distribution records, we identified the geographic provenance for mineral dust in each ice core through the

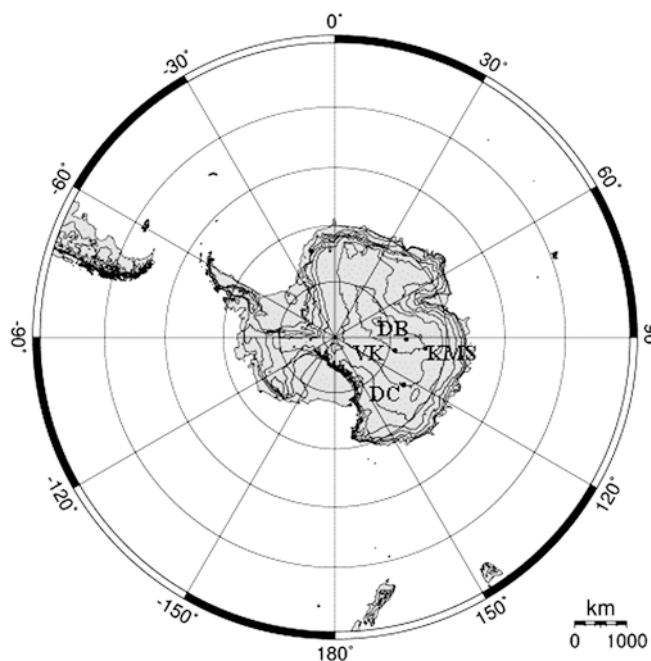


Fig. 1 Map of Antarctica with indication of the ice core drilling sites: Dome C (DC), DB (DB), Vostok (VK) and Komsomolskaia (KMS)

well-established geochemical method based on $^{87}\text{Sr}/^{86}\text{Sr}$ versus $^{143}\text{Nd}/^{144}\text{Nd}$ isotopic tracers.

2 Analytical techniques

2.1 The ice cores

The 780 m deep DB ice core (DB, 77°05'S, 94°55'E, 3650 m a.s.l.) was obtained during the 1987–1988 austral season by the 33rd Soviet Antarctic expedition. The site is located about 870 km from EDC, and has a similar ($\sim 3 \text{ g cm}^{-2} \text{ a}^{-1}$) accumulation rate (Jouzel et al. 1995). The climatic record and the chronology were published by Jouzel et al. (1995) along with a preliminary profile for dust concentration. This record covers the last 30 kyr.

The 885 m deep Komosmolskaia ice core (KMS, 74°05'S, 97°29'E, 3500 m a.s.l.) was extracted in 1983 during the 28th Soviet Antarctic Expedition. The accumulation rate for the Holocene is about $5 \text{ g cm}^{-2} \text{ a}^{-1}$; the time scale for this core was established by Ciais et al. (1992) and the climatic record by Jouzel et al. (2001). The record goes back in time only until 16 kyr BP, corresponding to the mid climatic transition.

The 788 m EDC core (75°06'S, 123°21'E, 3233 m a.s.l.) has been described by Jouzel et al. (2001) for the climate record over the last 27 kyr; the ice core chronology was established by Schwander et al. (2001), and the first dust profile for the LGM to Holocene transition produced by Delmonte et al. (2002a) is documented at higher resolution in this work.

2.2 Samples for dust concentration and size distribution measurements

The ice samples from the three ice cores were selected from sections corresponding to the period from 10 to 20 kyr BP. For each core the total number of samples analysed, the depth interval and the temporal frequency of sampling are reported in Table 1. All samples measure 5–6 cm in length and represent ~ 3 years of accumula-

tion. The procedure for sample preparation and decontamination is described in detail elsewhere (Delmonte et al. 2002a). Measurements were performed in random order using a microparticle counter (Coulter Counter Multisizer IIe ©, 256-channels) set up in the class 100 clean room of LGGE-CNRS laboratory (Grenoble, France), and calibrated with a $2.07 \mu\text{m}$ latex. The instrument was set to detect particles with equivalent spherical diameter from 0.7 to $20 \mu\text{m}$. Each concentration and size distribution value represents the average of at least three independent measurements on the same sample. The total mass of insoluble dust has been calculated from the volume size distribution assuming an average density of 2.5 g cm^{-3} . Laboratory blanks were checked after each sample analysis and the average value was around 1 ppb.

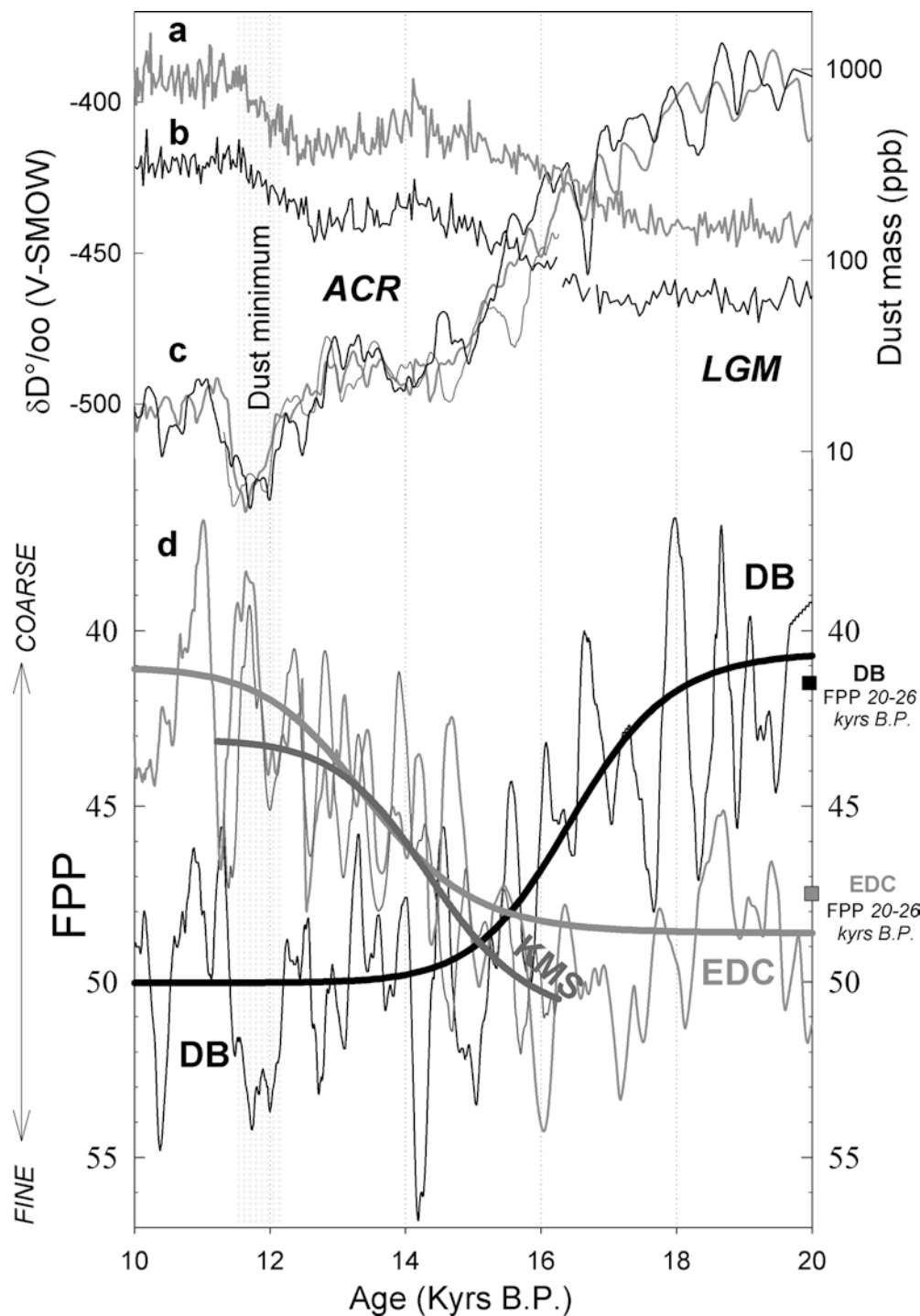
The mass-size distribution of aeolian particles in east Antarctica is usually well sorted around a mean mass diameter of $\sim 2 \mu\text{m}$ and the largest particle diameter is $\sim 5 \mu\text{m}$. The contribution of particles smaller than $0.7 \mu\text{m}$ represents less than $\sim 10\%$ of the total mass. The mass-size distribution can be fitted with a Lognormal or a Weibull function (Delmonte et al. 2002a), and the modal value of the regression can be adopted as indicator for particle dimensions. However, if the fitting properly smoothes the data, it reduces also the variability of the signal, particularly important when dealing with very low concentrated samples (see for example Fig. 3d-f).

To overcome this inconvenience we introduce a different indicator here for dust size, calculated directly from the raw data without mathematical fit: the proportion of fine particles (fine particle percentage, or FPP) or coarse particles (coarse particle percentage, or CPP) with respect to the total mass. The size intervals used for fine or coarse dust can be arbitrary chosen, provided that the upper limit of FPP is smaller than the modal value of the distribution ($\sim 2 \mu\text{m}$) and the lower limit of CPP is higher. In this work we calculated the FPP parameter in the interval from 1 to $2 \mu\text{m}$. Actually, the pattern of the three profiles obtained (Fig. 2) is rather insensitive to the interval selected, as far as the limitation stated above is respected.

Table 1 Ice samples and dust concentration measurements. Number of samples and relative depth interval, frequency of sampling (each sample being representative of ~ 3 years of accumulation). Mean dust concentration for each climatic period: LGM, ACR, pre-Holocene dust minimum and beginning of Holocene period

Ice Core	Number of samples	Sampling depth (m)	Sampling frequency (sample/year)	Dust concentration (ppb)			
				Late LGM (18–20 kyr BP)	ACR (14.5–12.2 kyr BP)	Pre-Holocene dust minimum (11.3–12.1 kyr BP)	Beginning Holocene (10–11.3 kyr BP)
DB	186	360–609	1/52	854	46	7	18
KMS	102	662–870	1/50	nm	25	9	nm
EDC	138	322–500	1/53 from 10 to 14.5 kyr BP 1/100 from 14.5 to 20 BP	730	25	8	18

Fig. 2 Climate and dust records for the deglaciation **a, b**: Stable isotopes profiles of EDC ice core (*light gray*) from Jouzel et al. (2001) and DB ice core (*black line*) from Jouzel et al. (1995). **c**: Dust concentration records from DB (*black line*) EDC (*light gray line*) and KMS (*dark gray line*) smoothed with a 200-yr running average. **d**: Dust FPP records (fine particle percent, see text) from DB (*black line*) EDC (*light gray line*) and KMS (*dark gray line*) ice cores. Lines correspond to the 200-years running average; in bold the mean trend of each series is reported. The *squares* on the *right-hand side* indicate the average FPP for DB and EDC ice cores during the LGM



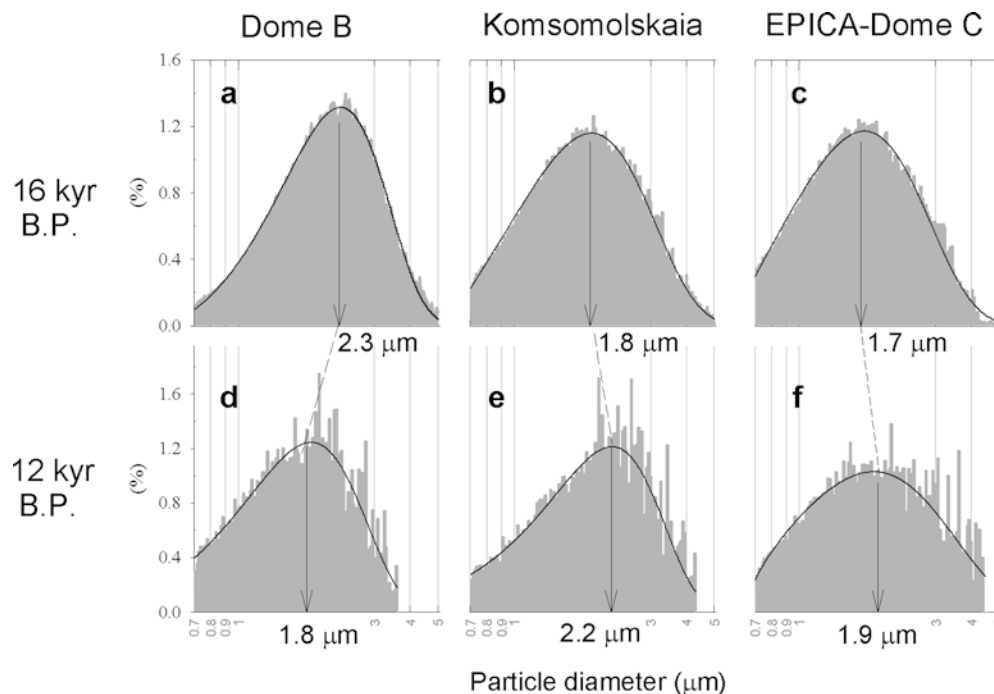
2.3 Samples for Sr-Nd isotopic measurements

Two samples for each site have been selected for $^{87}\text{Sr}/^{86}\text{Sr}$ and $^{143}\text{Nd}/^{144}\text{Nd}$ isotopic analysis. For the DB and EDC ice cores they were taken from the LGM period, while for the KMS core they were taken from the climatic transition.

Sample preparation involved decontamination of the samples through three repeated washings in ultra-pure (MilliQ) water in a class 100 clean room (LGGE-CNRS,

Grenoble). The mineral fraction was extracted by centrifugation as in Basile (1997). The evaporation method used in previous studies (Grousset et al. 1992; Basile et al. 1997) was not adopted in this work in order to avoid possible Sr contributions from marine aerosols. After centrifugation, the supernatant of the samples was removed using a syringe and bottom samples gathered for a next centrifugation. The final bottom liquid (~ 20 – 30 ml from about 300 – 900 g initial sample) was evaporated. The total mass of dust collected, estimated by

Fig. 3 Examples of normalized volume (mass) size distributions around 16 and 12 kyr BP. The volume-size distribution corresponds to the average of three to four adjacent samples selected around 16 and 12 kyr BP. The raw data were fitted by using a four-parameters Weibull function; the *mode* of the distribution is also indicated



Coulter Counter from final sample, was very low and variable (a factor 10) among the samples from $\sim 10 \mu\text{g}$ to $\sim 100 \mu\text{g}$ (Table 2).

Coulter Counter measurements gave evidence for residual and very diluted particles in the supernatant, whose size distribution was identical to the whole initial sample. This observation suggested an overall lack of size differentiation induced by the centrifugation and a probable absence of mineralogical (hence isotopic) differentiation. However, a test was made by analysing the isotopic composition of particles from the supernatant of a DB sample collected by filtration.

The chemical procedures for Sr and Nd separation and the isotopic measurements were performed at the Cosmochemistry Department of the Max-Planck-Institute in Mainz, Germany. The laboratory procedures are described in detail by Bogdanovski (1997). The separation of Sr and Nd has been done through ionic exchange columns. The total amount of Sr and Nd collected was calculated assuming an average upper continental crust

(UCC) concentration for both elements (350 ppm and 26 ppm respectively, Taylor and McLennan 1985), and a $\sim 95\%$ efficiency for each passage through the columns. Laboratory blanks were lower than 20 pg for both elements.

The extremely low amounts of Sr and Nd extracted are reported in Table 2 and span from $\sim 3 \text{ ng}$ to $\sim 40 \text{ ng}$ for Sr and from ~ 0.2 to 3 ng of Nd. Isotopic analyses on such small amounts require a highly-sensitive thermo-ionization mass spectrometer (TIMS) like the one we used in this study; it was especially set up for small terrestrial and extraterrestrial samples by Dr. E. Jagoutz (MPI, Mainz; see Bogdanovski 1997). Before measurements, the samples were put at $\sim 800 \text{ }^\circ\text{C}$ for 10–12 h to enhance the sample purification and improve the signal. Then, they were heated slowly up to 1200–1300 $^\circ\text{C}$ for measurements. Each sample measurement was made over a duration of ~ 17 –24 h and the Sr and Nd isotopic ratios that are reported represent the average of ~ 600 individual ratios (Table 3).

Table 2 Ice samples for isotopic composition measurements: sample code, ice core sections selected and relative climatic period. The modal value of the mass size distribution of each sample is also reported, along with the net ice weight (after decontamination) and

total dust recovered estimated by Coulter Counter after centrifugation procedures. The amount of Sr and Nd are also estimated and reported in the last two columns

Sample	Depth (m)	Climatic period	Mode of mass-size distribution (μm)	Sample Weight (grams)	Dust (μg)	Sr recovered (ng)	Nd recovered (ng)
EDC-a	518.10–518.65 520.30–520.85	Stage 2	~ 69 –2	690	~ 65 –70	22.30	1.66
EDC-b	569.80–570.35	Stage 2	~ 2.0	280	~ 100	34.30	2.55
DB-a	581	Stage 2	~ 2.7 –2.8	110	110	37.73	2.80
DB-b	641	Stage 2	~ 2.4 –2.5	860	100	34.30	2.55
KMS-a	850.08–851.23	Deglaciation	~ 2.2	800	10	3.43	0.25
KMS-b			~ 2.0	870	30	10.29	0.76

Table 3 Sr and Nd isotopic composition of ice core dust: $^{87}\text{Sr}/^{86}\text{Sr}$, $^{143}\text{Nd}/^{144}\text{Nd}$ and $\epsilon_{\text{Nd}}(0)$ from this study: each value represents the weighted average of a number of ratios for each element indicated in the last two columns

Sample	$^{87}\text{Sr}/^{86}\text{Sr}$	$^{143}\text{Nd}/^{144}\text{Nd}$	$\epsilon_{\text{Nd}}(0)$	Number of Sr ratios	Number of Nd ratios
EDC-a	0.708595 (21)	0.512553 (27)	-1.66 (0.53)	600	570
EDC-b	0.708834 (37)	0.512512 (32)	-2.46 (0.62)	385	604
EDC-b repeated	0.709033 (81)			980	
DB-a	0.708383 (32)	0.512608 (18)	-0.59 (0.35)	675	213
DB-a repeated	0.708316 (39)			760	
DB-a-filtered	0.708479 (18)	0.512613 (28)	-0.49 (0.55)	600	733
DB-b	0.708544 (28)	0.512526 (29)	-2.18 (0.57)	540	715
KMS-a	0.708493 (22)	0.512563 (51)	-1.46 (0.99)	245	680
KMS-b	0.709058 (38)	0.512484 (99)	-3.00 (1.93)	165	680

The Neodymium isotopic composition is expressed as $\epsilon_{\text{Nd}}(0)$, defined as:

$$\epsilon_{\text{Nd}}(0) = \left(\frac{(^{143}\text{Nd}/^{144}\text{Nd})_{\text{meas}}}{(^{143}\text{Nd}/^{144}\text{Nd})_{\text{CHUR}}} - 1 \right) \times 10^4$$

where the $^{143}\text{Nd}/^{144}\text{Nd}$ ratio for the CHUR (Chondritic Uniform Reservoir) is 0.512638 (Jacobsen and Wasserbrug 1980). The measured $^{143}\text{Nd}/^{144}\text{Nd}$ ratios have been corrected for mass fractionation by normalising to $^{146}\text{Nd}/^{144}\text{Nd} = 0.7219$, while the $^{87}\text{Sr}/^{86}\text{Sr}$ ratios have been normalised to $^{86}\text{Sr}/^{88}\text{Sr} = 0.1194$.

3 Results

3.1 The dust concentration profiles

The dust concentration records for the three ice cores are shown in Fig. 2c (running average over about 200 years) along with the profiles of stable isotopes from DB and EDC. The time period investigated spans the end of the LGM and the climatic transition until the beginning of the Holocene (20 to 10 kyr BP). The KMS record is shorter and covers the climatic transition from about 16.4 BP to 11.2 kyr BP.

The microparticle concentration profiles from the three ice cores are remarkably similar, and the general trends covariate almost synchronously without time scale adjustments. The mean particle concentrations for each climatic period is shown in Table 1. The very high levels characterizing the LGM (850 ppb at DB and 730 ppb at EDC respectively) started to decrease rapidly around 18 kyr BP, reaching the very low values typical for the Holocene around 14.5 kyr BP. A shallow re-increase of dust concentration then follows between 14.5 and 12.2 kyr BP, in concomitance to the Antarctic Cold Reversal (ACR). At this time, the particle concentration at the three sites is about twice the mean Holocene level. After a decrease following this event, a well-marked period with extremely low dust concentrations (~ 7 – 9 ppb) and spanning 800–1000 years (from about 11.3 to 12.1 kyr BP) is evident in the three records. Such a *pre-Holocene dust minimum* is very important both for its climatic implications and because it represents a very useful stratigraphic marker among the ice cores.

3.2 The dust size distribution records

The FPP records for the three ice cores are shown in Fig. 2d (moving average over ~ 200 years), along with the long-term trend of the changes (bold lines). The main trends of particle size changes during the climatic transition highlights two important phenomena: first, the opposite evolution of the dust size parameter between DB, on one side, and EDC-KMS on the other; second, the different timing and duration of the changes. Moreover, the evolution of the dust size displays some short-term (millennial to secular scale) oscillations over the period studied.

During the late LGM, from 18 to 20 kyr BP, dust at DB is characterised by high proportions of relatively large particles and, conversely, by a lower quantity of fine particles (FPP $\sim 41\%$, modal value $\sim 2.4 \mu\text{m}$). At the same time, EDC dust is marked by the opposite characteristics: i.e., the dust is relatively fine (modal value $\sim 1.9 \mu\text{m}$, FPP $\sim 48\%$), as already noted by Delmonte et al. (2002a). Indeed this difference between the two sites already existed during the preceding millennia (since ~ 26 kyr BP), as documented by a set of 12 additional samples from DB giving low FPP values ($\sim 41.5\%$ on average) and by 45 additional samples from EDC giving FPP of $\sim 47.3\%$ on average.

The change from coarse LGM dust sizes to finer particles begins around 18 kyr BP at DB, and is almost synchronous with the large reduction of the total dust concentration. At this site, the size changes operate over ~ 3 – 4 kyr until about 14.5 kyr BP, when average Holocene size particles (FPP $\sim 50\%$) are reached. The timing of the dust size changes is different at EDC, starting around 16 kyr BP, spanning a time period of ~ 5 – 6 kyr and reaching the average Holocene values (FPP $\sim 41\%$) around 10.5 kyr BP. Interestingly, the KMS particle size profile for the climatic transition is tightly similar to EDC. At 15 kyr BP the FPP for the three dust records are comparable.

In order to give an idea of the differences in particle size distributions from site to site and for the different climatic periods, we averaged the dust size distributions of 3–4 adjacent samples from each ice core around 16 and 12 kyr BP; the results are shown in Fig. 3. Between 16 and 12 kyr BP, the average mode of DB decreases from $\sim 2.3 \mu\text{m}$ to $\sim 1.8 \mu\text{m}$ (Fig. 3a, d), while at the

same time the dust mode increases from $\sim 1.8 \mu\text{m}$ to $\sim 2.2 \mu\text{m}$ at KMS (Fig. 3b, e) and from $\sim 1.7 \mu\text{m}$ to $\sim 1.9 \mu\text{m}$ (Fig. 3c, f) at EDC respectively.

All records show that the main trend of FPP changes at each site is overlaid by multi-centennial to millennial-scale fluctuations. The sampling resolution is almost constant in depth for the three ice cores, but as the accumulation rate significantly changed during the deglaciation, the time resolution of the samples gradually decreases with depth; this prevents us from performing an accurate spectral analysis. For the purpose of this study we just limited to the visual observation that the minimum values of the short-term fluctuations are separated by periods of 600–700 years. Due to the lack of stratigraphic markers, it is difficult to evaluate the phasing of millennial-scale fluctuations; however, when such a marker is available, during the pre-Holocene dust minimum, then the FPP profiles exhibit as clear antiphase.

3.3 The dust Sr-Nd isotopic signature

The $^{87}\text{Sr}/^{86}\text{Sr}$ versus $^{143}\text{Nd}/^{144}\text{Nd}$ isotopic ratios are reported in Fig. 4a, b and in Table 3. The isotopic signature of the samples is almost identical and spans a very narrow interval between $0.708316 < ^{87}\text{Sr}/^{86}\text{Sr} < 0.709058$ and $-3 < \epsilon_{\text{Nd}}(0) < -0.45$. Figure 4a and the greater detail in Fig. 4b show that the ice-core dust (ICD) isotopic field for the LGM is extremely restricted

even taking the error bars into account. The isotopic signature of the DB sample obtained by filtering the supernatant (#DB-a-filtered) and that of particles extracted by centrifugation ($\Delta^{87}\text{Sr}/^{86}\text{Sr} \sim 0.000096$ and $\Delta\epsilon_{\text{Nd}}(0) \sim 0.097$) are almost identical, thus confirming that the extraction procedure used is reliable and does not generate mineralogical and isotopic fractionation inside the sample.

Figure 4b also shows for comparison, the Sr-Nd isotopic values of an LGM *old* Dome C ice-core dust sample analyzed by Basile (1997), that matches our data very well.

4 Discussion

The dust input (flux) in Antarctica depends on many factors, which can be classified into three main categories. First the source strength, including soil properties, vegetation cover and factors influencing the quantity of particles available for deflation (Tegen et al. 2002); second, the processes occurring *en route* and linked to the hydrological cycle; third, the transport. Processes occurring *en route* are mainly the wet and dry deposition processes (Tegen and Fung 1994), affecting the mean residence time of the particles in the air.

At polar latitudes and in east Antarctica the dominant deposition process is the dry deposition (Legrand and Mayewski 1997). The residence time of the mineral

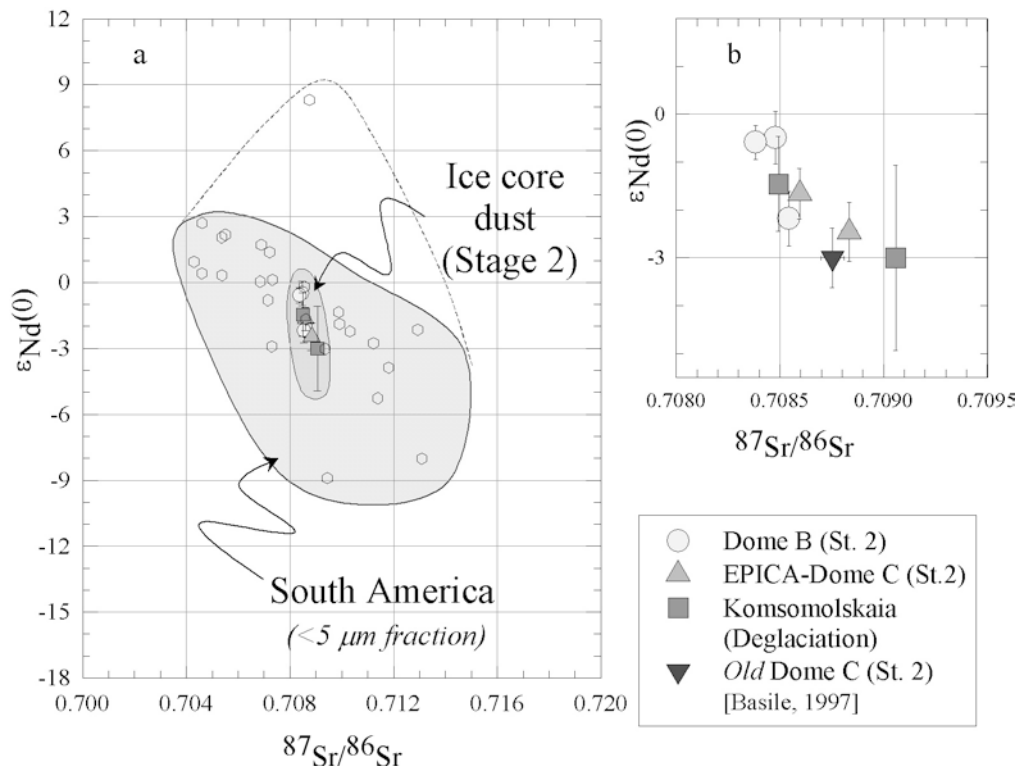


Fig. 4 Sr and Nd isotopic signature for the ice-core dust and South America: **a** comparison between the isotopic field for ice-core dust and southern South America samples (from Delmonte et al. 2004). **b** Zoom on LGM and deglaciation ice-core isotopic signature from DB, EDC and KMS with error bars

aerosol in the atmosphere is also size-dependent, and for particles with diameters between 1.6 and 3 μm it has been estimated to be $\sim 180\text{--}220$ h (Tegen and Fung 1994). Finally, the transport medium also plays a key role, both in terms of transit time between the source and the sink, and in terms of transport pathway for aerosol through the troposphere. Interestingly, the dust size distribution depends mainly on transport conditions.

4.1 The geographical provenance of dust

The dust isotopic signature appears almost identical among the three ice cores (Fig. 4a, b), giving evidence for a common dust provenance for the three sites and probably to the whole of the east Antarctic plateau. The same conclusion was drawn by Delmonte et al. (in press) for cold stages 2, 4 and 6 from dust isotopic investigations performed on EDC and Vostok ice cores. In this latter study, the isotopic signature of dust in ice cores was compared to the signature of potential source areas (PSAs) from the Southern Hemisphere continents. The Sr-Nd signature of the PSAs was measured on the grain size fraction equivalent to the dust that is transported long range (i.e. on the < 5 μm fraction), in order to prevent size-dependent isotopic fractionation.

Southern South America ($> 31^\circ\text{S}$ of latitude) was confirmed as the dominant dust source for EDC and Vostok during cold periods, as previously proposed by Grousset et al. (1992) and Basile et al. (1997). The isotopic ratios of the < 5 μm fraction of loess and aeolian samples from the Pampas, Patagonia and Chile are shown in Fig. 4a for comparison; the excellent match between the LGM dust isotopic signature and the southern South American one (Fig. 4a) nicely confirms the same conclusion for DB and KMS sites as well.

4.2 The dust concentration records

The dust concentration changes from the late LGM to the beginning of the Holocene period (20 to 10 kyr BP) show parallel evolution at DB, DC and KMS sites, giving evidence for an overall uniformity of dust input to the east Antarctic plateau. Since the accumulation rate at DB and EDC sites is almost the same (Jouzel et al. 1995) the dust fluxes are also comparable.

The features of the dust changes initially depicted in a first EDC dust record at low resolution (Delmonte et al. 2002a) are now characterized in better detail and confirmed by the DB and the KMS records. The shallow further increase of dust concentration accompanying the ACR phase and the pre-Holocene dust minimum, in particular, were both interpreted as possible changes in environmental conditions in the dust source regions (Delmonte et al. 2002a). The ACR dust event probably reflects a return to cooler conditions during the last termination. As largely discussed elsewhere (Delmonte

et al. 2002a), however, paleo-environmental indicators from the high latitudes of the Southern Hemisphere do not all confirm this hypothesis.

The pre-Holocene dust minimum on the other hand, is thought to be primarily related to the hydrological cycle, either in terms of increased humidity at the source (e.g. a humid period in South America) and weakening of its strength, or in terms of increased scavenging *en route* by wet deposition (Delmonte et al. 2002b). As the dominant dust provenance is likely the same for the whole east Antarctic plateau, the pre-Holocene dust minimum is probably a climatic event affecting the dust input over all east Antarctica, and a very important marker for stratigraphic correlations.

4.3 The regional differences of dust transport during LGM

The general covariance of the particle concentration records during the last climatic transition contrasts markedly with the opposite regional evolution of dust size. The relatively small size of EDC LGM particles was interpreted as an enhanced isolation of the Dome C site from meridional penetration of air masses (Delmonte et al. 2002b). The new data from DB and KMS allow us to complete the picture for the $94^\circ\text{E}\text{--}123^\circ\text{E}$ sector of east Antarctica, showing a clear regional variability at mesoscale. The enhanced isolation of some sites during the glacial period occurred in tandem with preferential incursions of dust-carrying air masses towards other sites on the plateau. For the drilling site of Vostok, located ~ 300 km far from DB, particle size data are available for the Holocene period (Delmonte 2003) and some from the LGM (Briat et al. 1982), but the deglaciation is not documented. Nevertheless, particles at Vostok appear coarser during the LGM than in the Holocene, and at first order more similar to DB.

The LGM dust is characterised by significant differences in particle size between the DB and EDC ice cores, and from 20 to 18 kyr BP the Δ FPP is $\sim 7\%$ (corresponding to difference in mode $\Delta\mu \sim 0.5$ μm). The KMS core does not cover this climatic period. However, its evolution is closely similar to EDC during the deglaciation suggesting the same similarity holds for the LGM.

The regional differences of particle size can be, in principle, the result of different transport times (t). In turn, this could reflect either (1) a contribution from two or more independent sources at different distance and leading to different transit times for aerosols, or (2) different wind speeds of the dust-carrying air masses from the source(s) to the sites, or (3) different dust trajectories from a common source. Since the geographic provenance of mineral aerosol is the same for the three sites (See Sect. 4.1) and the processes occurring “*en route*” (dry/wet deposition processes) are likely the same, then hypotheses 1 and 2 can be reasonably discarded and aerosol trajectories in the troposphere have to be considered. According to Ruth et al. (2003), when

all parameters of transport are identical (dry deposition mechanisms and velocity, mixing heights, and comparable size distributions), the transit time (t) from the source to the sink may be deduced directly from the dust mode. Longer or shorter t , in turn, can be related to different atmospheric pathways.

The DB to EDC ratio for the dust mode (μ_{DB}/μ_{DC})_{LGM} is ~ 1.26 for the LGM and the transit time ratio between the two sites (t_{DB}/t_{DC})_{LGM} that can be derived from Ruth et al. (2003) is ~ 0.6 – 0.8 , depending on different scenarios. In other words, the time of dust transport from South America to EDC can be estimated to be ~ 1.25 to ~ 1.7 times longer than to DB, assuming wind speeds are the same. A similar proportion is deduced for the length of the respective atmospheric trajectories. With respect to the long-range transport from southern South America to east Antarctica, the ~ 870 km distance between DB and EDC sites can hardly explain the large size differences observed. Therefore, air masses must have followed very different pathways to reach the sites.

GCM simulations for dust during the LGM suggest a preferential pathway for dust reaching Antarctica. The modelled seasonal dust flux in the Southern Hemisphere during the LGM (Andersen 1998) for the austral spring (September to November) shows a possible dust advection from Patagonia to the east Antarctic either through short-cut trajectories around the Weddel sea and onto the Queen Maud Land or via longer and more zonal circumpolar paths. The author gave evidence that dust flux lines from Patagonia enter the Antarctic from about 45°E during LGM and about 80°E during the present-day, a conclusion that may account for LGM dust at the DB site. Indeed, difficulties arise when interpreting the Early Holocene period during which EDC would have to be on a short-cut trajectory with respect to DB, while it is located to the east of DB and more downwind with respect to the general atmospheric circulation.

4.4 A scenario for the dust grading: effect of the altitude of the pathway to Antarctica

The dust size differences observed can be attributed to a different pathway for dust, that has to be considered in a three-dimensional space. The size of the mineral aerosol in the atmosphere decreases with height (Tegen and Lacis 1996) and the higher the altitude reached by dust, the longer the residence time.

For dust transport to Antarctica, the effect can be well illustrated by the dissemination and transport of volcanic products such as ash and gases (mostly SO_2) after an eruption. Visible ash layers are sometimes present in ice cores, which may contain volcanic particles as large as $50\ \mu\text{m}$. Such very large particles are carried to Antarctica through a tropospheric path. On the other hand, H_2SO_4 spikes in ice reflect a pathway through the stratosphere, where SO_2 is converted in to sulfuric acid.

Here we give an example of a volcanic event (~ 3.5 kyrs BP) detected by a strong acidic spike in a Vostok ice core around 130 m depth (Fig. 5). The tropospheric transport (first arrival) is represented by a sharp increase in both the total dust concentration and size. The value rises to ~ 3 – $4\ \mu\text{m}$, becoming significantly higher than background levels. Microscopic observations allowed us to identify volcanic particles by dark minerals and small glass shards. After this first phase, a huge spike of sulfuric acid can be clearly observed. This second phase corresponds to the stratospheric dust arrival. At the culmination of this second phase, the dust concentration is still significant but the modal value drops to ~ 1.5 – $1.7\ \mu\text{m}$, i.e. well below background levels that will be re-established later.

Due to its cold surface, Antarctica acts as a large thermal anticyclone with divergent wind fields over the surface and, at altitude, a large low-inducing upper air convergence and sinking (subsidence, see James 1989). The advection from layers above the inversion over Antarctica, for example, leads to a shallow temperature rise during winter time, responsible for the “coreless winters” (Schwerdtfeger 1984).

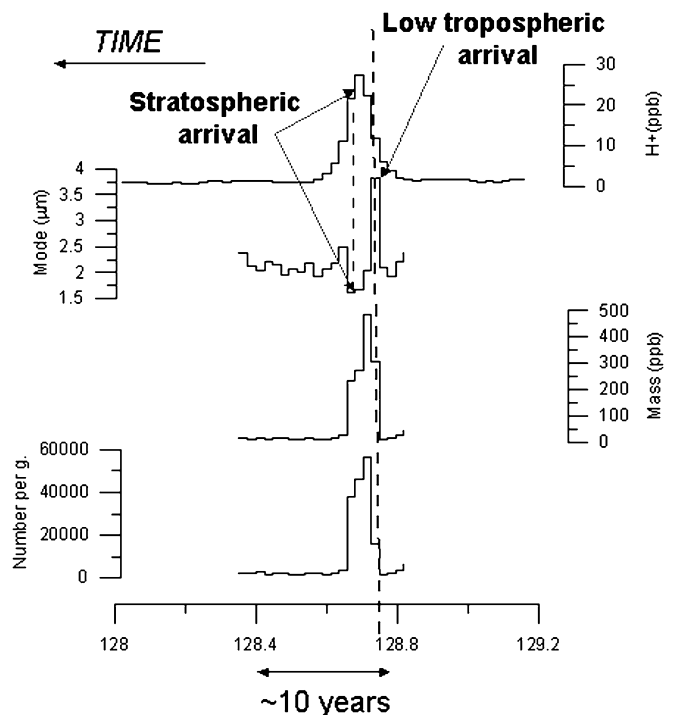


Fig. 5 Evolution of dust characteristics in correspondence to a volcanic event on Vostok ice core. Record versus depth (meters below the surface) of: *upper right*, H^+ concentration (ppb) mostly from H_2SO_4 as deduced from the ionic balance of the samples; *upper left*, mode (μm) of the dust size distribution; *lower right* dust mass concentration (ppb); *lower left* number concentration (N. per ml). The event around 128 m occurred circa ~ 3.5 kyr BP. Time goes from *right to left*. The tropospheric (first) and the stratospheric (second) arrivals are associated with dust with very different size characteristics

For the dust emitted into the troposphere from the continents around Antarctica, the local advection of mid-to-high troposphere air masses (higher than 4000 m a.s.l and likely up to the tropopause) is made possible by deep lows at altitude. Subsequently, air subsidence from different tropospheric levels may lead to a variable grading of dust reaching the interior of Antarctica, smaller particles being associated with a preferential subsidence from upper air levels and larger particles, conversely, with lower paths within the troposphere.

4.5 A sketch for evolution of the subsidence strength during the last climatic transition

The climatic changes associated with the LGM-Holocene transition, such as the reduction of the sea-ice extent and the weakening of the meridional temperature gradient implied a general reorganization of the atmospheric circulation in the circumAntarctic (e.g. Jouzel et al. 1995).

If the covariance of the dust input suggests a general uniformity of the net dust transport poleward, the conversed regional evolution of the particle size during the last climatic transition, and the asynchronous timing and duration of the changes, clearly highlight a meso-scale diversity of dust transport patterns.

As pointed out in Sect. 4.4, small-sized dust with a long atmospheric residence time is probably carried through upper troposphere air masses, that subside

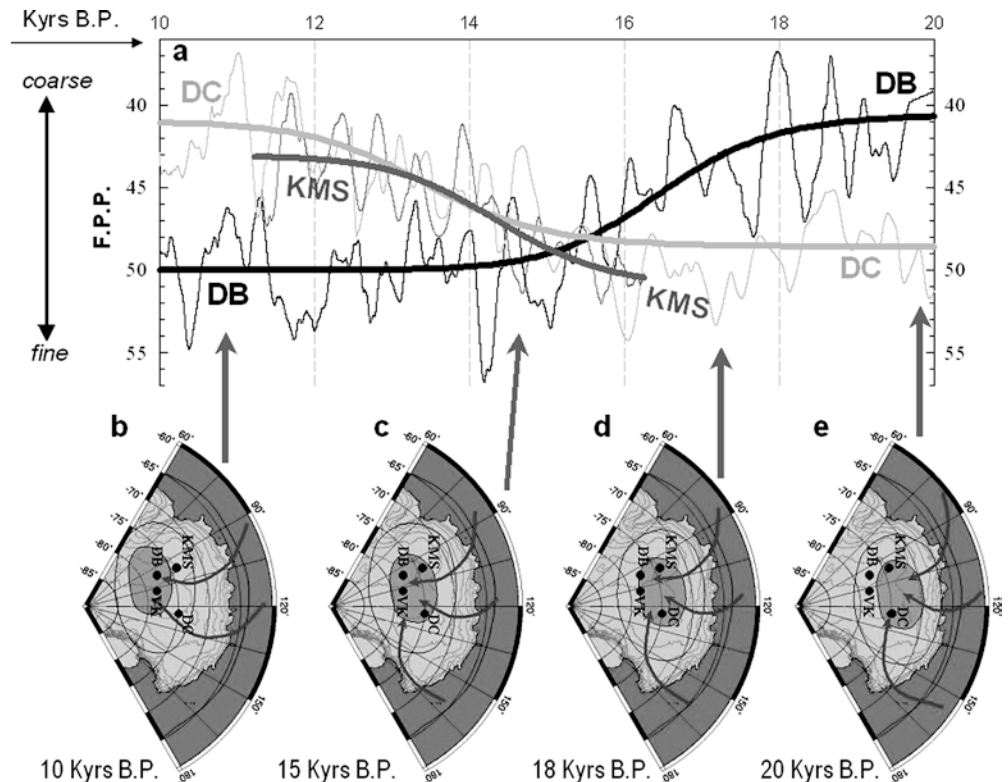
preferentially over certain areas. The very low temperatures during the LGM made subsidence more pronounced every where in Antarctica compared to the Holocene. Our data, however, suggest that during the LGM a preferential upper air subsidence would have covered the EDC-KMS region, when DB and probably Vostok were under influence of air from relatively lower levels and probably advected through short-cut trajectories.

The changes that occurred during the last climatic transition, following this interpretation, would reflect atmospheric circulation arrangements from a late glacial state with subsidence occurring preferentially over the EDC-KMS area (Fig. 6e), to an Early Holocene state when the zone of preferential subsidence moved over DB and Vostok (Fig. 6b).

The timing of the changes suggests that at ~ 18 kyr BP (Fig. 6e) the vortex over EDC and KMS probably started to expand or to shift southward towards DB and Vostok (Fig. 6d). This time period corresponds also to the beginning of the drastic LGM/Holocene dust concentration reduction. Around 15 kyr BP, at the end of the LGM dust reduction, all sites were likely under the same circulation regime (Fig. 6c). The southward migration of the vortex seemed to have continued until the beginning of the Holocene (Fig. 6b).

The scenario proposed suggests progressive southward displacement of the polar vortex during the last climatic transition, in other terms a change in the eccentricity, intended as distance of the central position of the vortex from the geographic pole.

Fig. 6 Sketch of the vortex migration during the deglaciation: **a** dust size evolution at the three sites, as in Fig. 2d. **b–e** Average position of the areas of preferential upper air convergence and subsidence over central east Antarctica suggested by the data. After the LGM, at 18 kyr BP the vortex probably expanded or shifted southwards towards the DB region. At about 15 kyr BP all sites were likely under the same circulation regime. The displacement continued until 10 kyr BP, corresponding to the beginning of the Holocene



4.6 Supporting evidences

In addition to this study, there is only limited evidence for regional differences in the atmospheric transport over Antarctica. Vimeux et al. (1999, 2001) study that used deuterium excess as proxy for reconstructing the temperatures of the oceanic moisture source for Vostok, suggested that such sources were located at lower latitudes during the last glacial period than during the Holocene and that meridional transport was enhanced. Observing the variations in the deuterium excess profile calculated at Dome C, Stenni et al. (2001) supported the idea that the ocean sources supplying moisture to Vostok and Dome C could be different, at least in the Holocene.

Moreover, a recent study on snow accumulation rates at EDC and Vostok spanning the last 40 kyr (Udisti et al. in press) suggests glacial to Holocene relative changes that could be linked to the influence of the vortex. The EDC/Vostok accumulation rate ratio for the Holocene was estimated as ~ 1.4 and only close to 1 for the last glacial period. This means that accumulation rate was higher at Vostok and/or smaller at EDC during the last glacial period, in response to a different transport regime and advection of air masses, with different humidity, to the two sites. Indeed, our dust size data suggest that over the EDC region high-altitude air mass advection is likely to have occurred during the LGM, and a probable negative anomaly in the accumulation rate should to be expected at this site. At the same time in contrast, the Vostok region would have been influenced by lower altitude and relatively wetter airmasses, coarser dust particles and a positive anomaly in snow accumulation.

4.7 The sub-millennial oscillations

Some short-term oscillations with periodicity of ~ 600 – 700 years (Fig. 2d) are evident in all three records, superposed on the main trend of dust size changes associated with the vortex migration. Millennial and centennial-scale periodicities of dust size variability have already been shown for the late deglaciation and Holocene periods from the EDC ice core (Delmonte et al. 2002b). The Antarctic vortex has been a permanent pattern of the Earth's atmospheric circulation since the beginning of the Quaternary period and its variability is spread over a large spectrum of periodicities, from daily to glacial/interglacial cycles.

Spectral analyses (not shown) of each record indicate that millennial and secular-scale oscillations are significant with respect to a red noise signal. An important point for our purpose is that millennial oscillations also appear in the opposite phase during the pre-Holocene dust minimum, suggesting that regional diversity of circulation regimes can occur at higher frequencies than those associated to the glacial/interglacial changes. In order to test the scenario proposed, GCM simulations of

the polar vortex and air subsidence with adequate spatial resolution over east Antarctica are needed at this stage.

5 Conclusions

The general uniformity of the mineral dust provenance and flux to East Antarctica during the last climatic transition masks the significant differences of dust transport pathways that can be depicted through the particle size distributions.

Dust size data from three ice cores in the 94°E – 123°E sector of East Antarctica show clearly a bipolar mode of variation during the last climatic transition. During the LGM, upper air convergence and sinking dominated in the EDC-KMS area, while DB and probably Vostok were under the influence of lower-level air masses with shorter trajectories. The progressive changes occurred between 20 and 10 kyr BP are interpreted as a gradual change in the eccentricity of the polar vortex. The presence of ubiquitous and out-of-phase secular and millennial scale dust size oscillations superposed on the main trend of the changes, moreover, points out that regional differences in the atmospheric circulation regime may exist also at these timescales.

Model simulations of the polar vortex and air subsidence zoomed over different sectors of the southern polar region are necessary to test this scenario.

Acknowledgements B. Delmonte thanks the Scientific Committee for Antarctic Research (SCAR) for awarding her the Prince of Asturias Fellowship 2003.

K.K. Andersen thanks the Carlsberg foundation for financial support. Thanks to V. Masson-Delmotte and anonymous reviewers for their useful suggestions that allowed us to improve the manuscript. This work is a contribution to the "European Project for Ice Coring in Antarctica" (EPICA), a joint ESF (European Science Foundation)/EC scientific programme, funded by the European Commission under the Environmental and Climate Programme (1994–1998) contract ENV4-CT95-0074 and by national contributions from Belgium, Denmark, France, Germany, Italy, the Netherlands, Norway, Sweden, Switzerland and the United Kingdom.

References

- Andersen KK (1998) Simulations of atmospheric dust in the glacial and interglacial climate. PhD Thesis, Niels Bohr Institute of Astronomy, Physics and Geophysics, University of Copenhagen, Copenhagen, pp 136
- Basile I (1997) Origine des aérosols volcaniques et continentaux de la carotte de glace de Vostok (Antarctique). PhD Thesis, LGGE-Université Joseph Fourier-Grenoble I, Grenoble, pp 254
- Basile I, Grousset FE, Revel M, Petit JR, Biscaye PE, Barkov NI (1997) Patagonian origin of glacial dust deposited in East Antarctica (Vostok and Dome C) during glacial stages 2, 4 and 6. *Earth Planet Sci Lett* 146: 573–589
- Bogdanovski O (1997) Development of highly-sensitive techniques for Sm-Nd isotopic analysis and their application to the study of terrestrial and extraterrestrial objects. PhD Thesis, Cosmochemistry Department Max Plank Institute, Johannes Gutenberg Universität, Mainz, Germany

- Briat M, Royer A, Petit JR, Lorius C (1982) Late glacial input of eolian continental dust in the Dome C ice core: additional evidence from individual microparticle analysis. *Ann Glaciol* 3: 27–30
- Carleton AM (1989) Antarctic sea-ice relationships with indices of the atmospheric circulation of the Southern Hemisphere. *Clim Dyn* 3: 207–220
- Ciais P, Petit JR, Jouzel J, Lorius C, Barkov NI, Lipenkov V, Nicolaiev V (1992) Evidence for an early Holocene climatic optimum in the Antarctic deep ice-core record. *Clim Dyn* 6: 169–177
- Delmonte B (2003) Quaternary origin and variations of continental dust in East Antarctica. Ph.D Thesis, University of Siena (Siena, Italy)-Université Joseph Fourier-Grenoble I (Grenoble, France), p 274
- Delmonte B, Petit JR, Maggi V (2002a) Glacial to Holocene implications of the new 27,000-year dust record from the EPICA Dome C (East Antarctica) ice core. *Clim Dyn* 18: 647–660
- Delmonte B, Petit JR, Maggi V (2002b) LGM-Holocene changes and Holocenemillennial-scale oscillations of dust particles in the EPICA Dome C ice core, east Antarctica. *Ann Glaciol* 35: 306–312
- Delmonte B, Basile-Doelsch I, Petit JR, Maggi V, Revel-Rolland M, Michard A, Jagoutz E, Grousset F (2004) Comparing the EPICA and Vostok dust records during the last 220 000 years: stratigraphical correlation and origin in glacial periods. *Earth Sci Rev* (in press)
- Grousset FE, Biscaye PE, Revel M, Petit JR, Pye K, Jossau S, Jouzel J (1992) Antarctic (Dome C) ice-core dust at 18 ky BP: isotopic constraints and origins. *Earth Planet Sci Lett* 111: 175–182
- Jacobsen SB, Wasserburg GJ (1980) Sm-Nd isotopic evolution of chondrites. *Earth Planet Sci Lett* 50: 139–155
- James IN (1989) The Antarctic drainage flow: implications for hemispheric flow on the Southern Hemisphere. *Antarctic Science* 1: 279–290
- Jouzel J, Vaikmae R, Petit JR, Martin M, Duclos Y, Stievenard M, Lorius C, Toots M, Melières MA, Burckle LH, Barkov NI, Kotlyakov VM (1995) The two-step shape and timing of the last deglaciation in Antarctica. *Clim Dyn* 11: 151–161
- Jouzel J, Masson V, Cattani O, Falourd S, Stievenard M, Stenni B, Longinelli A, Johnsen SJ, Steffensen JP, Petit JR, Schwander J, Souchez R (2001) A new 27 kyr high resolution East Antarctic climate record. *J Geophys Res* 28: 3199–3202
- King JC, Turner J (1997) Antarctic meteorology and climatology. Cambridge University Press, Cambridge, UK p 409
- Kohfeld K, Harrison SP (2001) DIRTMAP: the geological record of dust. *Earth Sci Rev* 54: 81–114
- Legrand M, Mayewski P (1997) Glaciochemistry of polar ice cores: a review. *Rev Geophys* 35: 219–243
- Mahowald N, Kohfeld K, Hansson M, Balkanski Y, Harrison SP, Prentice IC, Schulz M, Rodhe H (1999) Dust sources and deposition during the Last Glacial Maximum and current climate: a comparison of model results with paleodata from ice cores and marine sediments. *J Geophys Res* 104: 15,895–15,916
- Petit JR, Briat M, Royer A (1981) Ice Age aerosol content from East Antarctic ice core samples and past wind strength. *Nature* 293: 391–394
- Petit JR, Jouzel J, Raynaud D, Barkov NI, Barnola JM, Basile I, Bender M, Chappellaz J, Davis M, Delaygue G, Delmotte M, Kotlyakov VM, Legrand M, Lipenkov VY, Lorius C, Pépin L, Ritz C, Saltzman E, Stievenard M (1999) Climate and atmospheric history of the past 420 000 years from the Vostok ice core, Antarctica. *Nature* 399: 429–436
- Royer A, Angelis MD, Petit JR (1983) A 30 000 year record of physical and optical properties of microparticles from an East Antarctic ice core and implications for paleoclimate reconstruction models. *Clim Change* 5: 381–412
- Ruth U, Wagenbach D, Steffensen JP, Biggler M (2003) Continuous record of microparticle concentration and size distribution in the central Greenland NGRIP ice core during the last glacial period. *J Geophys Res* 108: 4098–4110
- Schwander J, Jouzel J, Hammer CU, Petit JR, Udisti R, Wolff E (2001) A tentative chronology for the EPICA Dome Concordia ice core. *Geophys Res Lett* 28: 4243–4246
- Schwerdtfeger W (1984) Weather and climate in the Antarctic, vol 15. Elsevier Science, Amsterdam, pp 261
- Stenni B, Masson-Delmotte V, Johnsen S, Jouzel J, Longinelli A, Monnin E, Röthlisberger R, Selmo E (2001) An oceanic cold reversal during the last deglaciation. *Science* 293: 2074–2077
- Taylor SR, McLennan SM (1985) The Continental crust: its composition and evolution, Blackwell Scientific Publications, Oxford, UK, pp 312
- Tegen I, Fung I (1994) Modeling of mineral dust in the atmosphere: sources, transport, and optical thickness. *J Geophys Res* 99: 22,897–22,914
- Tegen I, Lacis AA (1996) Modeling of particle size distribution and its influence on the radiative properties of mineral dust aerosol. *J Geophys Res* 101: 19,237–19,244
- Tegen I, Harrison SP, Kohfeld K, Prentice IC, Coe M (2002) The impact of vegetation and preferential source areas on global dust aerosol: results from a model study. *J Geophys Res* 107, doi:10.1029/2001JD000963
- Thompson LG, Mosley-Thompson E (1981) Microparticle concentration variations linked with climatic change: evidence from polar ice. *Science* 246: 812–815
- Udisti R, Becagli S, Castellano E, Delmonte B, Jouzel J, Petit JR, Schwander J, Stenni B, Wolff E (2004) Stratigraphic correlations between EPICA-Dome C and Vostok ice core showing the relative variations of snow accumulation over the past 45 kyr. *J Geophys Res* (in press)
- Van den Broeke MR (2000) The semi-annual oscillation and Antarctic climate, Part 4: a note on sea ice cover in the Amundsen and Bellingshausen Seas. *Int J Climatol* 20: 455–462
- Vimeux F, Masson V, Jouzel J, Stievenard M, Petit JR (1999) Glacial-interglacial changes in ocean surface conditions in the Southern Hemisphere. *Nature* 398: 410–413
- Vimeux F, Masson V, Delaygue G, Jouzel J, Petit JR, Stievenard M (2001) A 420 000 year deuterium excess record from east Antarctica: information on past changes in the origin of precipitation at Vostok. *J Geophys Res* 106: 31,863–31,873